

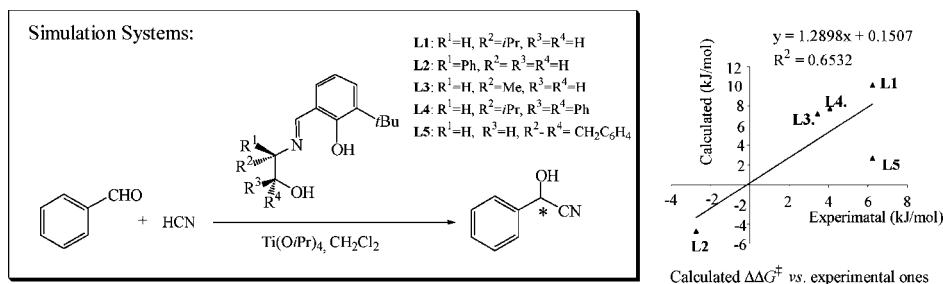
Computational Investigation on Stereochemistry in Titanium–Salicylaldehydes-Catalyzed Cyanation of Benzaldehyde

Song Qin, Changwei Hu,* Huaqing Yang, Zhishan Su, and Dianyong Tang

Key Laboratory of Green Chemistry and Technology, Ministry of Education, College of Chemistry, Sichuan University, Chengdu, Sichuan, 610064, China

gchem@scu.edu.cn

Received February 7, 2008



Theoretical simulation on the enantioselective cyanation of benzaldehyde over titanium–salicylaldehyde catalysts is performed with B3LYP//ONIOM methods. The calculations predict that the attack of cyanide to adsorbed benzaldehyde is the rate-determining step for the entire reaction. The stereochemistry of the titled reaction might be controlled not only by the attack directions of cyanide to benzaldehyde but also by different coordination modes of benzaldehyde to the chiral catalysts. In addition, to evaluate the accuracy of the employed method, the stereoselectivities of the reactions with five different chiral ligands are theoretically predicted. The theoretical predictions are qualitatively in agreement with experiments, and a linear relationship between calculated $\Delta\Delta G^\ddagger$ and experimental ones is obtained, especially for the reactions using the ligands with a single chiral center.

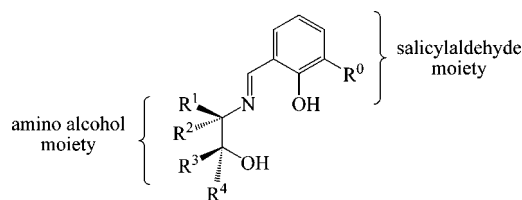
Introduction

C₁-symmetric chiral Schiff bases derived from the condensation of salicylaldehydes with suitable chiral amines are among the most successful types of ligands in organic synthesis (in Scheme 1), the metal complexes of which are enantioselective catalysts for important asymmetric processes, such as enantioselective Michael reactions,¹ Strecker reaction,² silylcyanation of aldehydes,^{3,4} addition of diketene⁵ and of diethylzinc⁶ to aldehydes, hydrophosphonylation of aldehydes,^{7,8} oxidation of sulfides,^{9,10} arylation of epoxides,¹¹ hetero-Diels–Alder reactions, and cyclopropanation of olefins.^{12–16}

Various authors employed these ligands with titanium tetraisopropoxide, Ti(OiPr)₄, to synthesize chiral titanium–salicylaldehyde catalysts for the cyanosilylation of benzaldehyde under mild reaction conditions.^{17–19} In 1993, Oguni and co-workers⁴ reported the synthesis and catalytic activity of the complexes derived from salicylaldehydes Schiff bases and Ti(OiPr)₄. The best results were obtained by using 20 mol % of the complex derived from ligand **L1** (i.e., R⁰ = *t*Bu; R² = *i*Pr; R¹ = R³ =

* Corresponding author. Phone: +86-28-85411105. Fax: +86-28-85411105.
 (1) Desimoni, G.; Quadrelli, P.; Righetti, P. P. *Tetrahedron* **1990**, *46*, 2927–2934.
 (2) Banphavichit, V.; Bhanthumnavin, W.; Vilaivan, T. *Tetrahedron* **2007**, *63*, 8727–8734.
 (3) Hayashi, M.; Miyamoto, Y.; Inoue, T.; Oguni, N. *J. Chem. Soc., Chem. Commun.* **1991**, 1752, 1753.
 (4) Hayashi, M.; Miyamoto, Y.; Inoue, T.; Oguni, N. *J. Org. Chem.* **1993**, *58*, 1515–1522.
 (5) Hayashi, M.; Inoue, T.; Oguni, N. *J. Chem. Soc., Chem. Commun.* **1994**, 341, 342.
 (6) Fleischer, R.; Braun, M. *Synlett* **1998**, 1441–1443.

(7) Ito, K.; Tsutsumi, H.; Setoyama, M.; Saito, B.; Katsuki, T. *Synlett* **2007**, 1960–1962.
 (8) Zhou, X.; Liu, X.; Yang, X.; Shang, D.; Xin, J.; Feng, X. *Angew. Chem., Int. Ed.* **2008**, *47*, 392–394.
 (9) Bolm, C.; Bienewald, F. *Angew. Chem., Int. Ed.* **1995**, *34*, 2640–2642.
 (10) Cogan, D. A.; Liu, G.; Kim, K.; Backes, B. J.; Ellman, J. A. *J. Am. Chem. Soc.* **1998**, *120*, 8011–8019.
 (11) Oguni, N.; Miyagi, Y.; Itoh, K. *Tetrahedron Lett.* **1998**, *39*, 9023–9026.
 (12) Dossetter, A. G.; Jamison, T. F.; Jacobsen, E. N. *Angew. Chem., Int. Ed.* **1999**, *38*, 2398–2400.
 (13) Gademann, K.; Chavez, D. E.; Jacobsen, E. N. *Angew. Chem., Int. Ed.* **2002**, *41*, 3059–3061.
 (14) Ruck, T. R.; Jacobsen, E. N. *J. Am. Chem. Soc.* **2002**, *124*, 2882–2883.
 (15) Cai, L.; Mahmoud, H.; Han, Y. *Tetrahedron: Asymmetry* **1999**, *10*, 411–427.
 (16) Li, Z.; Liu, G.; Zheng, Z.; Chen, H. *Tetrahedron* **2000**, *56*, 7187–7191.

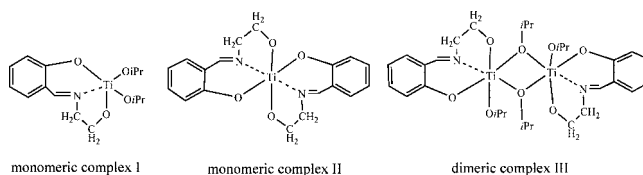
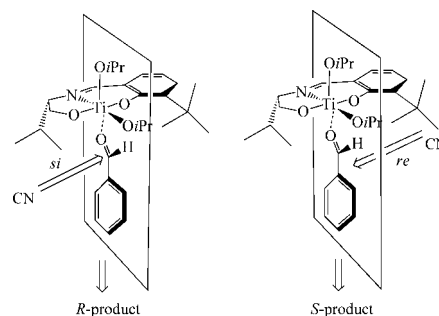
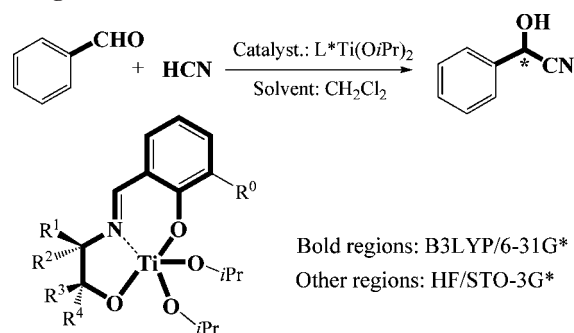
SCHEME 1. General Structure of C_1 -Symmetric Chiral Salicylaldehyde Schiff Base Ligands


$R^4 = H$) at $-80\text{ }^\circ\text{C}$ in dichloromethane. Jiang et al.^{20,21} showed that the titanium complex of Schiff bases would catalyze the conversion of aromatic aldehydes and cinnamaldehyde into *S*-cyanohydrins with 48–92% enantiomeric excess under the same reaction conditions used by Oguni. Somanathan and co-workers^{22,23} studied the use of Schiff bases derived from *cis*-1-amino-2-indanol as ligands to prepare the titanium-based catalysts for asymmetric cyanohydrin synthesis and determined the possible structures of the titanium–salicylaldehyde catalysts. Feng and co-workers²⁴ reported a series of titanium-complex catalysts derived from hydronated C_1 -symmetric Schiff bases for the cyanosilylation of various aliphatic, aromatic conjugated, and heteroaromatic aldehydes. The results gave excellent ee up to 94% with high yields of 90–99% under mild reaction conditions.

Experimental research offered several possibilities to explain the reaction mechanism and accumulated some useful information. You and co-workers supposed that hydrogen cyanide may be the real cyanation reagent²⁵ in silylcyanation of benzaldehyde over titanium-based catalyst. This cyanation reagent might be generated from TMSCN and HOiPr .⁴ In addition, the cyanide appeared to be transferred from TMSCN but not from titanium cyanide.²⁶

The explanation for the origin of its stereochemistry, however, is still in controversy. Especially, the details about the structure of the catalyst are uncertain so far. Prashar et al.²⁷ investigated the reaction of titanium isopropoxide with the Schiff base from salicylaldehyde and 2-hydroxyethylamine in different stoichiometric ratios (Scheme 2). They found that two monomeric (**I** and **II**) and one dimeric (**III**) species may be formed in their reaction and the formation of those species is closely dependent on reaction conditions (e.g., molar ratios, solvents, and ligands).

Oguni and co-workers⁴ measured field desorption (FD) mass spectra and the ^{13}C NMR spectrum of the alkoxy exchange reaction product of $\text{Ti}(\text{OiPr})_4$ and the Schiff base in different molar ratios. They detected the presence of monomeric complexes (**I**, **II**) in a 1:1 molar ratio mixture. They also noticed the low concentration of the dimeric compound and assumed

SCHEME 2. Three Products of Titanium Isopropoxide with the Schiff Base from Salicylaldehyde and 2-Hydroxyethylamine

SCHEME 3. The Mechanism with C_1 -Symmetric Titanium Complex for the *R* and *S* Product Formation Suggested by Oguni

SCHEME 4. Layering of the Catalytic Reaction System Derived from C_1 -Symmetric Chiral Salicylaldehyde Schiff Base Ligands


the dimeric compound to originate from the monomeric compound **I**. Besides, they found that the molecular weight of the catalyst ranges from 318 to 385 for the 1:1 molar ratio product of Schiff base and $\text{Ti}(\text{OiPr})_4$, which corresponds to the monomeric complex with one chiral ligand. On the basis of the above experimental data, Oguni and co-workers suggested a reaction model for such a high enantioselectivity based on the attack of an external nucleophile to the less hindered face of the adsorbed aldehyde (Scheme 3).

This model successfully explains the crucial role played by the *t*Bu substituent at the R^0 site in Schiff bases derived from *S*-configured 2-amino alcohols and salicylaldehyde in the blocking of the *re* face of the adsorbed aldehyde. Later, Somanathan, Walsh, and co-workers²² carried out extensive NMR studies to show that the presence of a large group at the R^0 position of the aromatic ring avoids the formation of inactive dimeric complex, or monomeric species with two chiral ligands. Hence, if R^0 is a large group (*t*Bu), the titanium complex formed from salicylaldehyde ligand may be a monomeric complex with pentacoordinate structure $[\text{L}^*\text{Ti}(\text{OiPr})_2]$.

To gain more details of the underlying elementary steps at a molecule level, some research based on computational chemistry

- (17) North, M. *Tetrahedron: Asymmetry* **2003**, *14*, 147–176.
 (18) Khan, N. H.; Kureshy, R. T.; Abdi, S. H. R.; Agrawal, S.; Jasra, R. V. *Coord. Chem. Rev.* **2008**, *252*, 593–623.
 (19) Ramón, D. J.; Yus, M. *Chem. Rev.* **2006**, *106*, 2126–2208.
 (20) Jiang, Y.; Zhou, X.; Hu, W.; Wu, L.; Mi, A. *Tetrahedron: Asymmetry* **1995**, *6*, 405–408.
 (21) Jiang, Y.; Zhou, X.; Hu, W.; Li, Z.; Mi, A. *Tetrahedron: Asymmetry* **1995**, *6*, 2915–2916.
 (22) Flores-Lopéz, L. Z.; Parra-Hake, M.; Somanathan, R.; Walsh, P. J. *Organometallics* **2000**, *19*, 2153–2160.
 (23) Gama, A.; Flores-Lopéz, L. Z.; Aguirre, G.; Parra-Hake, M.; Somanathan, R.; Walsh, P. J. *Tetrahedron: Asymmetry* **2002**, *13*, 149–154.
 (24) Li, Y.; He, B.; Qin, B.; Feng, X.; Zhang, G. *J. Org. Chem.* **2004**, *69*, 7910–7913.
 (25) Yang, F.; Wei, S.; Chen, C.-A.; Xi, P.; Yang, L.; Lan, J.; Gau, H.-M.; You, J. *Chem. Eur. J.* **2008**, *14*, 2223–2231.
 (26) Hamashima, Y.; Kanai, M.; Shibasaki, M. *J. Am. Chem. Soc.* **2000**, *122*, 7412–7413.
 (27) Prashar, P.; Tandon, J. P. *J. Less-Common Met.* **1967**, *13*, 541–547.

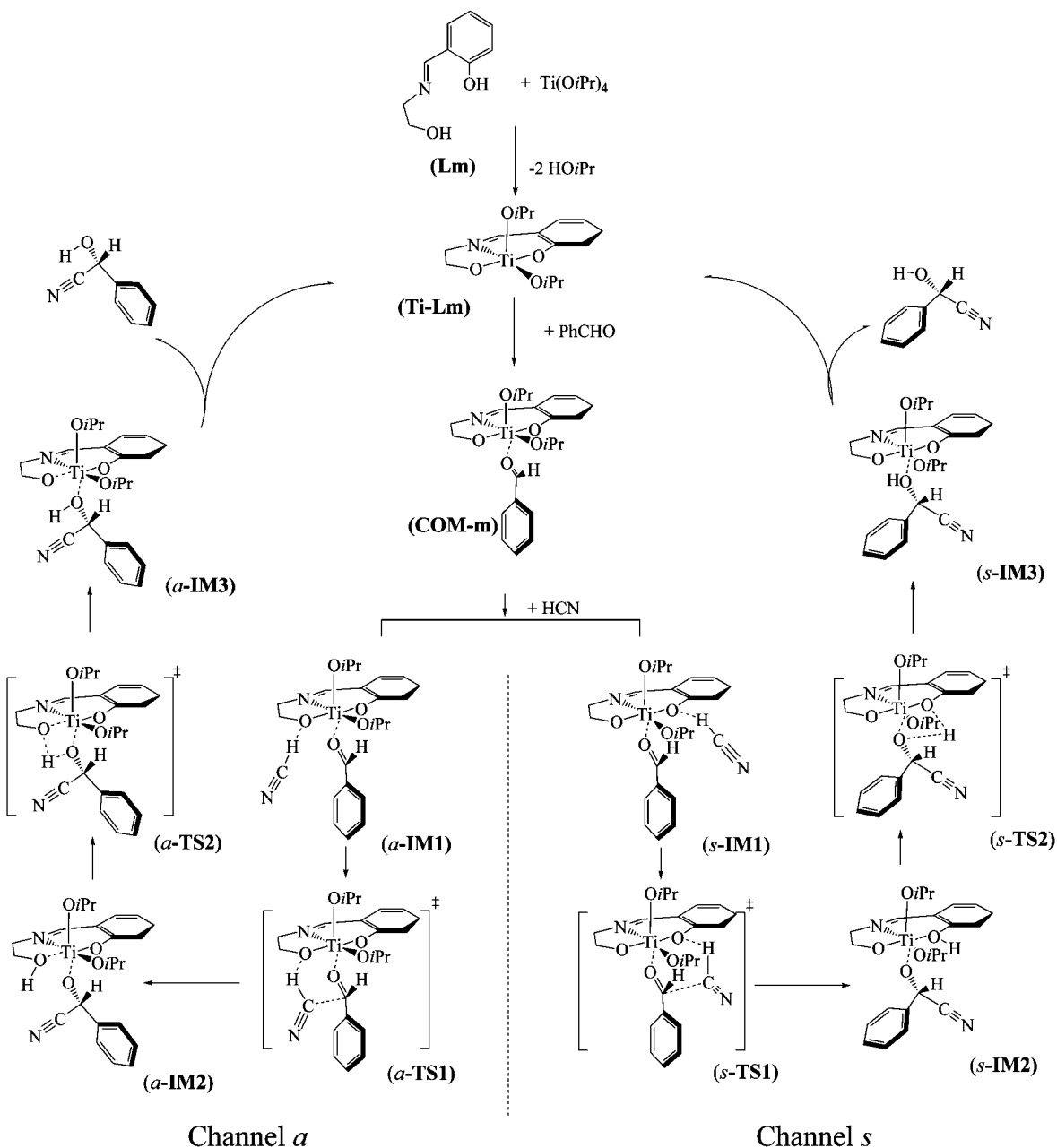


FIGURE 1. Predicted cyanation reaction mechanism over the modelled catalyst **Ti-Lm**. (The optimized geometries are listed in the Supporting Information.)

was done on this asymmetric reaction. Recently, Gama et al.²⁸ and Moyano and co-workers²⁹ performed fundamental calculations to investigate the stabilities of different monomeric species with one chiral ligand. Their results confirmed that the directions of cyanide attack play important roles in those high enantioselective reactions. Unfortunately, the theoretical explanation suggested by Moyano contradicted Oguni's model, although the ligands synthesized by both of them were comparable in experiments.

To our knowledge, however, there is no detailed reaction mechanism available in the literature, especially for the stereochemistry of such reactions. So it is difficult to evaluate the potential effects of chiral ligands, which hinders the design of

new effective chiral ligands theoretically. In an attempt to gain a better understanding of the reaction and provide clues to related asymmetric synthesis investigations, the present theoretical simulation aimed at the stereochemical nature of those reactions was carried out. This work is expected to be useful for the design of new catalysts based on chiral metal–salicylaldehydes.

It should be noted that the present simulation systems just involve the monomeric species with one chiral ligand. Although the above experiments are liable to support that monomeric titanium species would afford high enantioselectivities, it has not been proven that the active species is monomeric in all cases. There is literature evidence that this is not always the case. More

(28) Gama, Á.; Flores-López, L. Z.; Aguirre, G.; Parra-Hake, M.; So-manathan, R.; Cole, T. *Tetrahedron: Asymmetry* **2005**, *16*, 1167–1174.

(29) Merono, R. M.; Rosol, M.; Moyano, M. *Tetrahedron: Asymmetry* **2006**, *17*, 1089–1103.

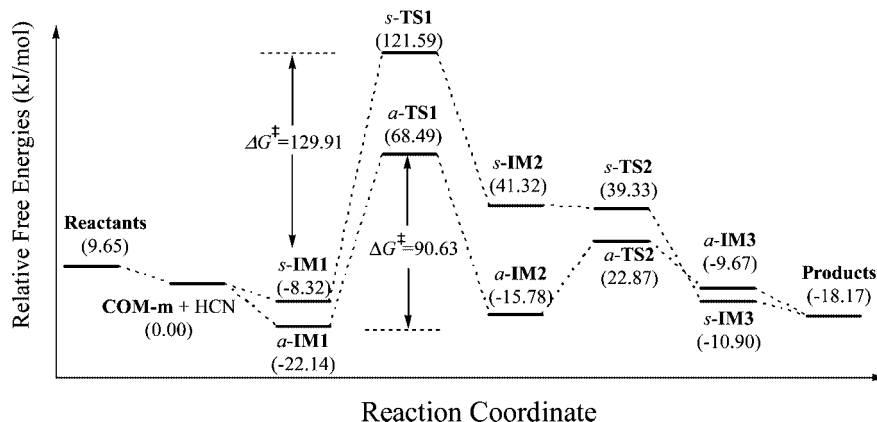


FIGURE 2. The relative free energy diagrams along the reaction pathway. Relative free energies (in kJ/mol) for various intermediates and transition states calculated at the B3LYP/6-311G** level are listed in parentheses.

TABLE 1. Total (in au) and Relative (in kJ/mol) Energies for Various Species along the Predicted Reaction Channels in the Modeled System

species	ONIOM(B3LYP:HF)		B3LYP(PCM, CH ₂ Cl ₂)	
	E_{total}	E_r	G_{total}	G_r
reactants ^a	-2220.518966	30.44	-2230.161031	9.65
COM-m + HCN	-2220.530566	0.00	-2230.164709	0.00
a-IM1	-2220.544100	-35.52	-2230.173147	-22.14
a-TS1	-2220.505049	66.96	-2230.138610	68.49
a-IM2	-2220.538466	-20.73	-2230.170722	-15.78
s-IM2	-2220.529025	4.04	-2230.155993	22.87
a-IM3	-2220.539317	-22.97	-2230.168400	-9.67
s-IM1	-2220.540359	-25.70	-2230.167880	-8.32
s-TS1	-2220.487700	112.50	-2230.118380	121.59
s-IM2	-2220.518519	31.62	-2230.148966	41.32
s-TS2	-2220.520314	26.91	-2230.149722	39.33
s-IM3	-2220.537944	-19.36	-2230.168863	-10.90
products ^b	-2220.526675	10.21	-2230.171633	-18.17

^a Reactants: Ti-Lm + HCN + benzaldehyde. ^b Products: Ti-Lm + cyanohydrin.

recently, Belokon et al.³⁰ developed a binuclear titanium complex derived from the hexadentate ligand and Ti(OiPr)₄. They found that the binuclear titanium complex is a more efficient catalyst for cyanation of aldehydes than its mononuclear analogues and considered that the dimeric titanium complexes should be the real catalysts. Nevertheless, they were not sure whether the dimeric model could be applied to the tridentate salicylaldehyde ligands, such as the structures depicted in Scheme 1. Because only one metal ion is involved in the present simulation, the present theoretical results may be relevant if the monomeric titanium complex is involved in the catalysis.

Computational Details

On the basis of the existing experimental data, the reaction shown in Scheme 4 is investigated. Regarding the computational costs, we employ ONIOM^{31–37} methods to simulate the asymmetric

reaction system in the present study, and the layering of the system is listed in Scheme 3. The internal region is treated with hybrid density functional theory B3LYP^{38–40} with the 6-31G* basis set.^{41–50} The remainder of the system is optimized at the HF/STO-3G* level. The bonds between atoms in the core and outer layers are broken and saturated by hydrogen atoms (link-atoms) for the higher level part of the ONIOM calculation on the core system.

Single-point B3LYP(PCM,⁵¹ CH₂Cl₂)/6-311G** calculations are performed on the optimized ONIOM structures. Each transition state is characterized by analysis of the normal mode corresponding to its unique imaginary frequency. All calculations are performed in the Gaussian 03 program package.⁵²

Results and Discussion

Reaction Mechanism over the Nonchiral Modeled Catalyst. Initially, a nonchiral ligand Lm is constructed wherein hydrogen atoms are used to substitute for R¹–R⁴ substituents and the R⁰ group. Then, this modeled ligand is used to interact with Ti(OiPr)₄ with the formation of the model titanium–salicylaldehyde catalyst Ti-Lm. This treatment is designed to probe the possible reaction channels in detail, especially to identify the rate-determining steps (RDS) for the entire cyanation reactions. The obtained reaction mechanism is shown in Figure 1. Total and relative energies for various species along the predicted reaction channels in the model system are listed in Table 1. The energy diagrams along the predicted reaction mechanism are depicted in Figure 2.

As shown in Figure 1, the B3LYP//ONIOM calculations feature two catalytic cycles (channel *a* and channel *s*, respectively), and both of them start from the formation of the benzaldehyde–catalyst complex COM-m. Considering there are several conformational states available to this complex, we initially tested the stabilities of its different conformations suggested by Oguni and Moyano. In Oguni's model, the adsorbed benzaldehyde is orientated with the aldehyde hydrogen

(30) Belokon, Y. N.; Chusov, D.; Borkin, D. A.; Yashkina, L. V.; Dmitriev, A. V.; Katayev, D.; North, M. *Tetrahedron: Asymmetry* **2006**, *17*, 2328–2333.

(31) Maseras, F.; Morokuma, K. *J. Comput. Chem.* **1995**, *16*, 1170–1179.

(32) Humbel, S.; Sieber, S.; Morokuma, K. *J. Chem. Phys.* **1996**, *105*, 1959–1967.

(33) Matsubara, T.; Sieber, S.; Morokuma, K. *Int. J. Quantum Chem.* **1996**, *60*, 1101–1109.

(34) Svensson, M.; Humbel, S.; Froese, R. D. J.; Matsubara, T.; Sieber, S.; Morokuma, K. *J. Phys. Chem.* **1996**, *100*, 19357–19363.

(35) Svensson, M.; Humbel, S.; Morokuma, K. *J. Chem. Phys.* **1996**, *105*, 3654–3661.

(36) Dapprich, S.; Komáromi, I.; Byun, K. S.; Morokuma, K.; Frisch, M. J. *THEOCHEM* **1999**, *462*, 1–21.

(37) Vreven, T.; Morokuma, K. *J. Comput. Chem.* **2000**, *21*, 1419–1432.

(38) Becke, A. D. *J. Chem. Phys.* **1993**, *98*, 5648–5652.

(39) Lee, C.; Yang, W.; Parr, R. G. *Phys. Rev. B* **1998**, *37*, 785–789.

(40) Miehlich, B.; Savin, A.; Stoll, H.; Preuss, H. *Chem. Phys. Lett.* **1989**, *157*, 200–205.

(41) Ditchfield, R.; Hehre, W. J.; Pople, J. A. *J. Chem. Phys.* **1971**, *54*, 724–728.

(42) Hehre, W. J.; Ditchfield, R.; Pople, J. A. *J. Chem. Phys.* **1972**, *56*, 2257–2261.

(43) Hariharan, P. C.; Pople, J. A. *Mol. Phys.* **1974**, *27*, 209–214.

(44) Gordon, M. S. *Chem. Phys. Lett.* **1980**, *76*, 163–168.

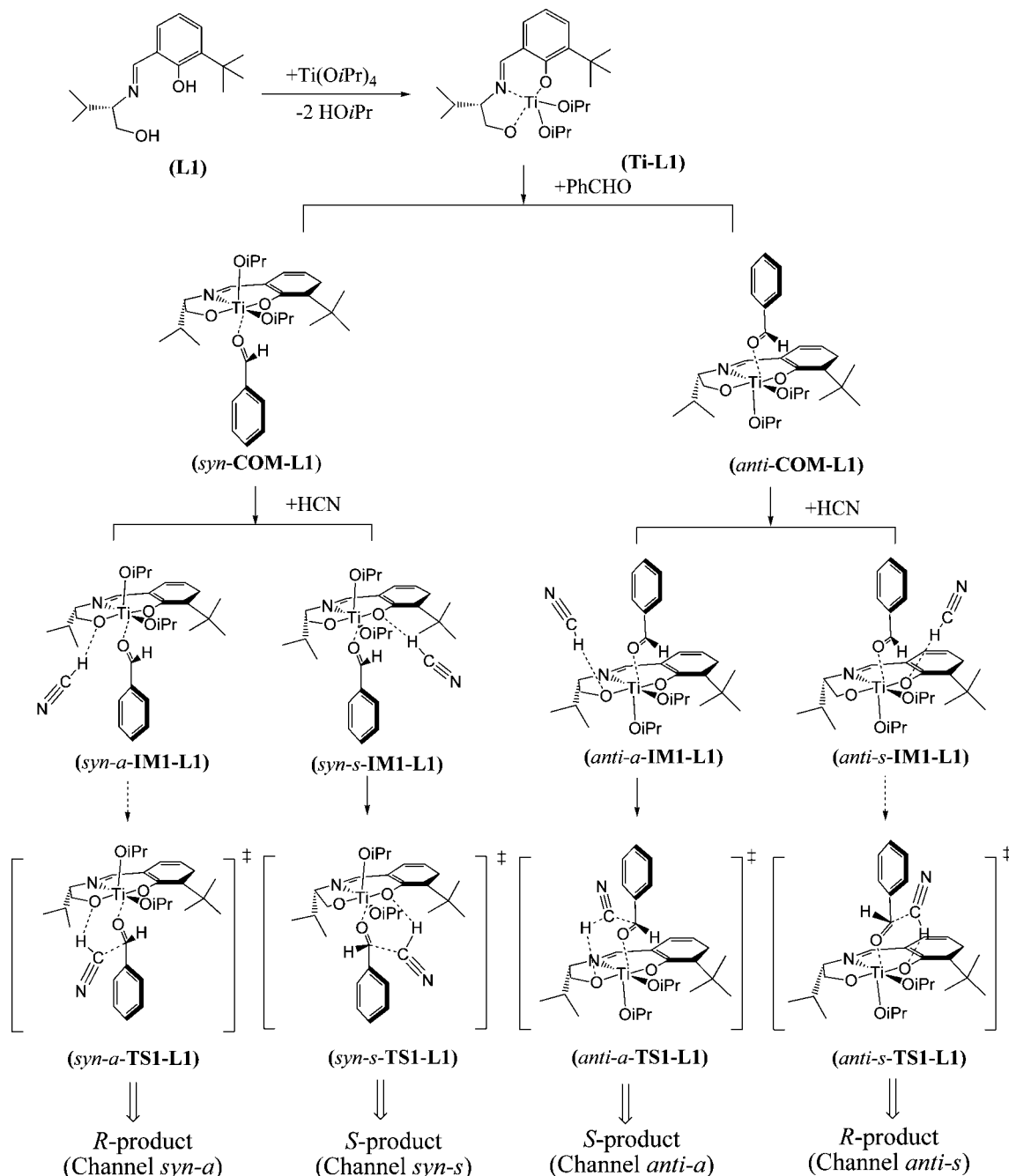


FIGURE 3. The asymmetric CN addition process over catalyst **Ti-L1** derived from chiral ligand **L1**.

pointed toward the isopropoxy group,⁴ while in Moyano's model, the adsorbed benzaldehyde is orientated with the aldehyde hydrogen pointed toward the Schiff base.²⁹ The structure suggested by Oguni is confirmed as an intermediate that could be formed from modeled catalyst **Ti-Lm** and free benzaldehyde with a stabilized energy of 9.65 kJ/mol at the B3LYP/6-311G** level. On the other hand, the structure suggested by Moyano cannot be identified as an energy minimum on the potential energy surface, as the geometry optimization for it always converges to Oguni's structure in our calculations.

(45) Hariharan, P. C.; Pople, J. A. *Theor. Chim. Acta* **1973**, *28*, 213–222.

(46) Blaudeau, J.-P.; McGrath, M. P.; Curtiss, L. A.; Radom, L. *J. Chem. Phys.* **1997**, *107*, 5016–5021.

(47) Francl, M. M.; Pietro, W. J.; Hehre, W. J.; Binkley, J. S.; DeFrees, D. J.; Pople, J. A.; Gordon, M. S. *J. Chem. Phys.* **1982**, *77*, 3654–3655.

With the benzaldehyde–catalyst complex **COM-m**, the reaction can occur along two reaction channels. As shown in Figure 1, along reaction channel *a*, an external HCN initially gets close to **COM-m** from the amino alcohol side, and then interacts with **COM-m** to form a co-complex *a-IM1* without any energy barrier. The following step is triggered by the attack of cyanide from the adsorbed HCN moiety to the carbonyl via transition state *a-TS1*, which leads to the formation of intermediate *a-IM2*. As a result, this reaction step cleaves the H–CN bond and the addition of CN to carbonyl is completed. Continuously, the hydrogen migration occurs via transition state *a-TS2* and yields the adsorbed cyanohydrin in intermediate *a-IM3*. Finally, the release of cyanohydrin takes place with the recovery of modeled catalyst. The calculations predict the highest ΔG^\ddagger for channel *a* to be 90.63 kJ/mol, which corre-

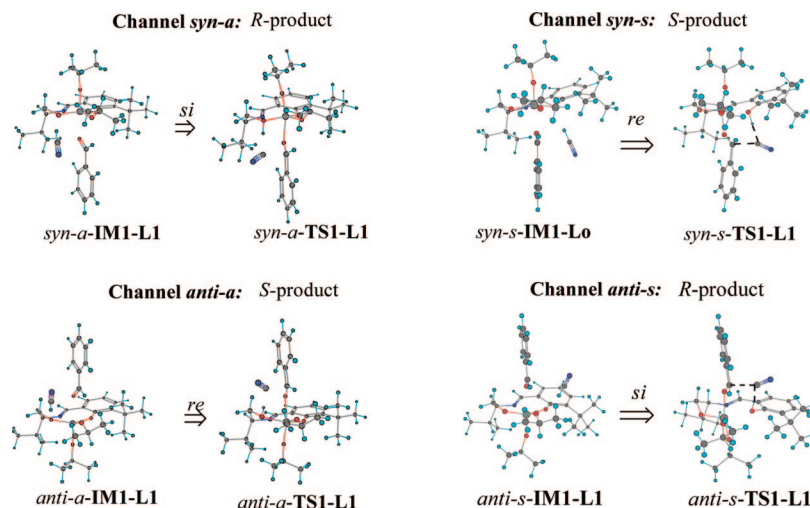


FIGURE 4. Intermediates and transition states along the four reaction channels over catalyst **Ti-L1**.

TABLE 2. Relative Free Energies (in kJ/mol) Obtained by Single-Point B3LYP/6-311G** Calculations for the Ligand **L1** System

channel	product config	G (IM1-L1)	G^\ddagger (TS1-L1)	ΔG^\ddagger	$\Delta\Delta G^\ddagger$
<i>syn-a</i>	<i>R</i>	0.00	80.08	80.08	0.00
<i>anti-a</i>	<i>S</i>	-6.61	83.58	90.19	10.11
<i>syn-s</i>	<i>S</i>	31.84	150.33	118.49	38.41
<i>anti-s</i>	<i>R</i>	30.07	156.70	126.63	46.55

sponds to the step from intermediate *a-IM1* to *a-IM2* via transition state *a-TS1*. This indicates that the rate-determining step for channel *a* should be the cyanide attack step. Hence, reaction channel *a* represents the attack of cyanide from the amino alcohol side.

On the other hand, as shown in Figure 1, there exists another reaction path marked as channel *s*. Along this reaction channel, an external HCN initially gets close to **COM-m** from the salicylaldehyde side, and then interacts with **COM-m** to form a co-complex *s-IM1* without any energy barrier. The following reaction steps are predicted similar with the reaction along channel *a*. The calculations predict the highest ΔG^\ddagger for this step to be 129.91 kJ/mol, which corresponds to the step from intermediate *s-IM1* to *s-IM2* via transition state *s-TS1*. Hence, reaction channel *s* represents the attack of cyanide from the salicylaldehyde side, as compared with channel *a*.

For both two reaction channels, the rate-determining steps are predicted to be the cyanide attack steps, which confirm that cyanide attack processes should be crucial to the entire reaction over titanium–salicylaldehyde catalysts. From the above data, the following conclusions can be drawn: (1) the attack process of cyanide is the rate-determining step in both channels and (2) remarkably, because ΔG^\ddagger for channel *a* is by 39.28 kJ/mol lower than that for channel *s*, reaction along channel *a* should be kinetically favored over that along channel *s*, which implies that the attack of cyanide from the amino alcohol side might be a predominant process for the reaction in the model system.

However, it should be noted that the modeled ligand, as well as its corresponding catalyst, is designed without any chiral centers. Although the above simulation successfully identifies the rate-determining steps for the cyanation reactions over the titanium–salicylaldehyde catalysts, the modeled nonchiral system cannot explain the stereochemistry of such reactions. Furthermore, the effects of R^1 – R^4 and R^0 substituents are not taken into account in the above model. Actually, those substitu-

ents have been proven very important for the asymmetric reactions in experiments. Those will be discussed in the next section.

The Asymmetric Cyanide Addition over the Chiral Catalyst. With the relatively simple structure and high enantioselective activity, the chiral ligand **L1** (in Figure 3) is employed to probe the origin of stereochemistry in this section. Ligand **L1** was developed by Oguni, where *t*Bu is introduced at the R^0 site and *i*Pr is linked at the R^2 site to generate a chiral center. This ligand is used to interact with $\text{Ti}(\text{O}i\text{Pr})_4$ to synthesize the chiral titanium–salicylaldehyde catalyst **Ti-L1**. This catalyst was reported to afford *R*-products from substituted aldehydes with enantioselectivities as high as 96%. The *R*-product from benzaldehyde was isolated in 67% yield and 85% ee in the presence of **Ti-L1** catalyst.⁴

As shown in Figure 3, if **Ti-L1** is used as the catalyst, the benzaldehyde–catalyst complex **COM-L1** allows two diastereotopic modes of coordination (*syn-COM-L1* and *anti-COM-L1*), due to the C_1 -symmetry of **COM-L1**. In *syn-COM-L1*, the *i*Pr constituent at the R^2 site is *syn* to the coordinated benzaldehyde; and in *anti-COM-L1*, this group is *anti* to the coordinated benzaldehyde. For each **COM-L1** (*syn* or *anti*), there are two different possibilities of interaction with HCN, and then this external cyanide attack can take place from the amino alcohol side (along channel *a*) and the salicylaldehyde side (along channel *s*), respectively. Consequently, four stereochemically different reaction channels result, marked as channels *syn-a*, *syn-s*, *anti-a*, and *anti-s* in Figure 3, respectively. The calculated relative free energies for RDS (from **IM1-L1** to **TS1-L1**) along four reaction channels are listed in Table 2, and the corresponding intermediates and transition states for *si* and *re* addition to benzaldehyde are depicted in Figure 4. The calculations predict that the *R*-cyanohydrin product should be formed in high ee, with *si* addition being preferred by 10.11 kJ/mol. According to absolute rate theory, the B3LYP single-point calculations give *R*-product formation with a selectivity of 96.7%.⁵³ Although this predicted result overestimates the experimental isolation of the *R*-cyanohydrin product in 85% ee, this theoretical prediction successfully reproduces the correct major product.

(48) Binning, R. C., Jr.; Curtiss, L. A. *J. Comput. Chem.* **1990**, *11*, 1206–1209.

(49) Rassolov, V. A.; Pople, J. A.; Ratner, M. A.; Windus, T. L. *J. Chem. Phys.* **1998**, *109*, 1223–1229.

Besides, as shown in Table 2, ΔG^\ddagger values of the reaction channels *syn-s* and *anti-s* are much higher (ca. 36 kJ/mol) than those of the other channels (*syn-s* vs *syn-a*; *anti-s* vs *anti-a*), which is comparable with the corresponding value (39.28 kJ/mol, channel *s* vs channel *a*) of the modeled catalyst **Ti-Lm**. This implies that the introduction of R^0-R^4 to the simplified model ligand does not remarkably change the relative energy barrier between the two attack directions of cyanide to adsorbed benzaldehyde. It is reasonable that the attack of cyanide from the amino alcohol side should be kinetically favored in the chiral ligand systems based on titanium–salicylaldehydes, and only two channels (*syn-a* and *anti-a*) are competing when relative free energies are considered. The competing lower energy asymmetric reaction steps can be summarized as the following: along channel *syn-a*, the cyanide attack may take place on the *si* face of benzaldehyde leading to the formation of *R*-cyanohydrin; along channel *anti-a*, the cyanide attack may take place on the *re* face of benzaldehyde leading to the formation of *S*-cyanohydrin.

Summarily, as suggested by Oguni⁴ and Moyano,²⁹ the attack directions of cyanide play important roles in the stereoselectivities of the reactions; meanwhile, the coordination modes of benzaldehyde to catalysts can also determine the stereoselectivities over the chiral titanium–salicylaldehydes. From a computational perspective, it becomes possible to simulate more chiral catalytic systems based on titanium–salicylaldehydes and to predict their stereoselectivities by means of theoretical calculations with lower computational costs.

The Accuracy of the Present Simulation on Stereochemistry. To confirm the above point of view and to determine the relative accuracy of the used methods, we turn our attention to the following four chiral ligands: ligands **L2–L4** with one chiral center and **L5** with two chiral centers (in Scheme 5), which were tested experimentally for silylcyanation of benzaldehyde under the same reaction conditions (reaction time: 36–40 h; temperature: -78 to -80 °C; catalyst concentration: 20% mol; solvent: CH_2Cl_2).

The treatments for the four ligands are similar with that of ligand **L1**. To give a concise expression, computational details, optimized structures, and relative energies are available in the Supporting Information. The theoretical $\Delta\Delta G^\ddagger$ from the calculated competing lower energy reaction channels and the experimental $\Delta\Delta G^\ddagger$ derived from ee values are listed in Table 3. In addition, a comparison between calculated and experimental stereoselectivities for the five chiral ligands is also carried out to determine the relative accuracy of the methods used.

(50) Rassolov, V. A.; Ratner, M. A.; Pople, J. A.; Redfern, P. C.; Curtiss, L. A. *J. Comput. Chem.* **2001**, *22*, 976–984.

(51) Cossi, M.; Scalmani, G.; Rega, N.; Barone, V. *J. Chem. Phys.* **2002**, *117*, 43–54.

(52) Frisch, M. J.; Trucks, G. W.; Schlegel, H. B.; Scuseria, G. E.; Robb, M. A.; Cheeseman, J. R.; Montgomery, J. A., Jr.; Vreven, T.; Kudin, K. N.; Burant, J. C.; Millam, J. M.; Iyengar, S. S.; Tomasi, J.; Barone, V.; Mennucci, B.; Cossi, M.; Scalmani, G.; Rega, N.; Petersson, G. A.; Nakatsuji, H.; Hada, M.; Ehara, M.; Toyota, K.; Fukuda, R.; Hasegawa, J.; Ishida, M.; Nakajima, T.; Honda, Y.; Kitao, O.; Nakai, H.; Klene, M.; Li, X.; Knox, J. E.; Hratchian, H. P.; Cross, J. B.; Bakken, V.; Adamo, C.; Jaramillo, J.; Gomperts, R.; Stratmann, R. E.; Yazyev, O.; Austin, A. J.; Cammi, R.; Pomelli, C.; Ochterski, J. W.; Ayala, P. Y.; Morokuma, K.; Voth, G. A.; Salvador, P.; Dannenberg, J. J.; Zakrzewski, V. G.; Dapprich, S.; Daniels, A. D.; Strain, M. C.; Farkas, O.; Malick, D. K.; Rabuck, A. D.; Raghavachari, K.; Foresman, J. B.; Ortiz, J. V.; Cui, Q.; Baboul, A. G.; Clifford, S.; Cioslowski, J.; Stefanov, B. B.; Liu, G.; Liashenko, A.; Piskorz, P.; Komaromi, I.; Martin, R. L.; Fox, D. J.; Keith, T.; Al-Laham, M. A.; Peng, C. Y.; Nanayakkara, A.; Challacombe, M.; Gill, P. M. W.; Johnson, B.; Chen, W.; Wong, M. W.; Gonzalez, C.; Pople, J. A. *Gaussian 03, B05*; Gaussian, Inc.: Wallingford, CT, 2003.

(53) Product ratios for the prediction were determined by converting ΔG^\ddagger_{298K} to ee by using absolute rate theory: $\ln(k_1/k_2) = -\Delta\Delta G^\ddagger/RT$.

SCHEME 5. Four Different Chiral Ligands Based on Salicylaldehydes

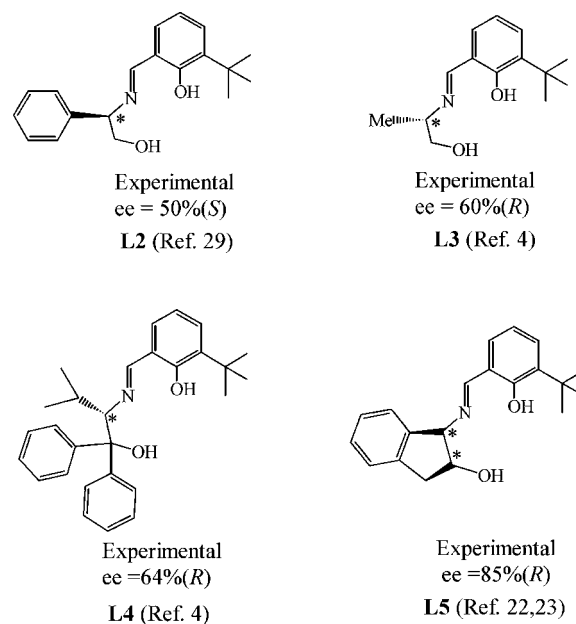


TABLE 3. $\Delta\Delta G^\ddagger$ (kJ/mol) and Configurations for Enantioselective Cyanation of Benzaldehyde^a

ligand	calculated		experimental	
	$\Delta\Delta G^\ddagger$	config	$\Delta\Delta G^\ddagger$	config
L1	10.11	<i>R</i>	6.23	<i>R</i>
L2	-4.74	<i>S</i>	-2.73	<i>S</i>
L3	7.19	<i>R</i>	3.44	<i>R</i>
L4	7.72	<i>R</i>	4.07	<i>R</i>
L5	2.71	<i>R</i>	6.23	<i>R</i>

^a The experimental activation free energies were derived from ee values in the literature. All free energies were calculated at 298.15 K and 1 atm.

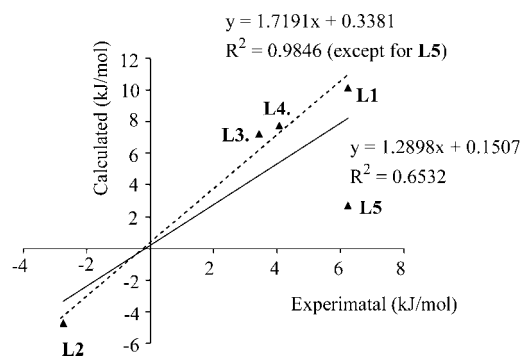


FIGURE 5. Graph of experimental $\Delta\Delta G^\ddagger$ versus calculated values for reactions involving ligands **L1–L5**.

Figure 5 is a graph of experimental versus calculated energies for ligands **L1–L5**.

As shown in Table 2 and Figure 5, although the selectivity for ligand **L5** is predicted lower than experimental value and the selectivities for the other four ligands are overestimated, the prediction is correct for the major product. The results indicate that the present novel mechanism is consistent with the major experimental observations and the existing explanation of stereochemistry for such asymmetric reactions. Hence, it is reasonable to consider that our computational methodology

represents a valuable method that should be an aid to the design of new asymmetric catalysts based on chiral metal–salicylaldehydes.

Conclusion

The calculations indicate that the attack process of cyanide is the rate-determining step for the entire reaction, and the cyanide attack can take place from the amino alcohol side and the salicylaldehyde side, respectively. The calculated ΔG^\ddagger implies that the attack of cyanide from the amino alcohol side should be a predominant process for such reactions.

The simulation on the chiral ligand system probes that the stereochemistry of the titled reaction might be controlled not only by the attack directions of cyanide but also by different coordination modes of benzaldehyde to the chiral catalysts. To determine the accuracy of the employed methods, theoretical simulation on five chiral ligands is carried out to discuss their stereochemistry in the cyanation of benzaldehyde. The theoretic-

cal predictions are qualitatively in agreement with experiments, and a linear relationship between calculated $\Delta\Delta G^\ddagger$ and experimental ones is also obtained, especially for the ligands with a single chiral center. The results indicate that the present novel mechanism is consistent with the major experimental observations and the existing explanation of stereochemistry for such asymmetric reactions. This computational methodology represents a valuable method that should be an aid to the design of new asymmetric catalysts based on chiral metal–salicylaldehydes.

Acknowledgment. The authors are gratefully for the financial support provided by NNSF of China (Nos. 20602026 and 20772085).

Supporting Information Available: Computational methods, geometries optimized, and the energies calculated. This material is available free of charge via the Internet at <http://pubs.acs.org>.

JO800316P